

Molecular dynamics simulation of nanofluid's flow behaviors in the near-wall model and main flow model

Chengzhi Hu · Minli Bai · Jizu Lv ·
Peng Wang · Liang Zhang · Xiaojie Li

Received: 18 July 2013 / Accepted: 23 December 2013 / Published online: 31 December 2013
© Springer-Verlag Berlin Heidelberg 2013

Abstract The flow behaviors of nanofluids were studied in this paper using molecular dynamics (MD) simulation. Two MD simulation systems that are the near-wall model and main flow model were built. The nanofluid model consisted of one copper nanoparticle and liquid argon as base liquid. For the near-wall model, the nanoparticle that was very close to the wall would not move with the main flowing due to the overlap between the solid-like layer near the wall and the adsorbed layer around the nanoparticle, but it still had rotational motion. When the nanoparticle is far away from the wall ($d > 11 \text{ \AA}$), the nanoparticle not only had rotational motion, but also had translation. In the main flow model, the nanoparticle would rotate and translate besides main flowing. There was slip velocity between nanoparticles and liquid argon in both of the two simulation models. The flow behaviors of nanofluids exhibited obviously characteristics of two-phase flow. Because of the irregular motions of nanoparticles and the slip velocity between the two phases, the velocity fluctuation in nanofluids was enhanced.

Keywords Nanofluids · Molecular dynamics method · Flow behaviors · Two-phase flow

1 Introduction

Nanofluids, which was first proposed by Choi (1995), are new heat transfer liquids with remarkable heat transfer capability prepared by suspending nanoparticles in traditional heat transfer liquids (water, ethylene glycol and engine oil). A mass of experiments demonstrated that the convective heat transfer coefficient of nanofluids is far higher than that of the base fluid whether in laminar or turbulent flow state condition (Duangthongsuk and Wongwises 2010; Heris et al. 2007; Ho and Chen 2013; Hwang et al. 2009; Wen and Ding 2004; Xuan and Li 2003). Therefore, nanofluids have wide application prospects in the heat transfer fields. For incompressible convective heat transfer, scalar field is determined by velocity field, that is, momentum transfer drives heat transfer. Therefore, the changes of flow characteristics is an important cause of heat transfer enhancement in nanofluids. Wen and Ding (2005) have speculated that the flow behaviors of nanofluids may impose an important effect on the heat transfer. In order to reveal the mechanisms of heat transfer enhancement in nanofluids, it is necessary to investigate the flow characteristics of nanofluids.

Many researches have been done on the flow behaviors of nanofluids by experimental and numerical simulation method. Xu et al. (2011) carried out visualization experiments on SiO_2 /water nanofluids in a wavy-walled tube and found that the flow of nanofluids is more active than that of the base liquid at the same Reynolds number. Beiki et al. (2013) investigated the turbulent mass transfer of Al_2O_3 and TiO_2 electrolyte nanofluids and found that the mass transfer coefficients of nanofluids are higher than that of the base fluid. The authors thought that the micro-convections produced by the nanoparticles are responsible for the increased mass transfer. Xuan and Roetzel (2000)

C. Hu · M. Bai · J. Lv (✉) · P. Wang · L. Zhang
School of Energy and Power Engineering, Dalian University
of Technology, Dalian 116024, China
e-mail: lvjizu@dlut.edu.cn

X. Li
The State Key Laboratory of Structural Analysis for Industrial
Equipment, Dalian University of Technology, Dalian 116024,
China

considered that nanofluids can be easily fluidized and the motion slip between the phases is negligible. Kalteh et al. (2011) and Haghshenas et al. (2010) used an Eulerian two-fluid model to calculate the laminar forced convection heat transfer in nanofluids. The results showed that the two-phase modeling approach predicts higher heat transfer enhancement than the single-phase model. He et al. (2009) and Bianco et al. (2009) used the single-phase model and Euler–Lagrange multiphase models to study the nanofluids convection heat transfer, respectively. They reported that the Euler–Lagrange model is more precise than the other one. Wang et al. (2013) used three different single-phase, Euler–Euler and Euler–Lagrange models to simulate nanofluids flow inside a wavy-walled tube. Their results showed that the Euler–Lagrange model is the most accurate. Based on these findings, we can conclude that the interactions between nanoparticles and a base fluid have an important influence on the convection heat transfer and cannot be ignored. The present traditional methods applied to compute the flow, heat transfer in nanofluids can only achieve micron level, and the interactions between the two phases could not be studied in detail.

Fortunately, molecular dynamics (MD) method, which is a computational method and solves molecular Newton equations of motion with known interatomic potentials, has proven an efficient method in investigating the micro-flow under shear flow condition (Jabbarzadeh et al. 1998, 2002; Thompson and Robbins 1990). Moreover, MD method provides an effective approach for the study of the interactions between nanoparticles and a base fluid. Vladkov and Barrat (2006) simulated the thermal properties of nanofluids by MD method and found that the molecular simulation is very flexible to study the thermal transfer between fluid and particle. Sarkar and Selvam (2007) employed MD method to compute the thermal conductivity of nanofluids and found that MD simulation is a very useful tool and can be used to study nanofluids thermal conductivity. Eapen et al. (2007) have studied the mechanism of thermal transport in nanofluids by combining linear response theory with molecular dynamics simulations. The results showed that the surface interactions are very important to the thermal conductivity enhancement of nanofluids. Li et al. (2008, 2010) investigated the molecular layering at the liquid–solid interface in nanofluids by molecular dynamics simulation. Their numerical results showed that an absorbed slip layer of liquid is formed at the interface between the nanoparticle and argon and it would move with the Brownian motion of the nanoparticle. Liang and Tsai (2011) demonstrated that the interfacial thermal resistance of molecular thin film confined between nanoparticles is depending on the film thickness by using non-equilibrium molecular dynamics simulations. Kang et al. (2011) investigated the mechanism of heat conduction in

nanofluids with molecular dynamics simulation, and a solid-like base fluid liquid layer around nanoparticles was found. Lin et al. (2011) calculated the thermophysical characteristics of nanofluids using MD method and found that the interfacial layer and nanoparticle size both have effect on the thermal conductivity enhancement of nanofluids. Mohebbi (2012) calculated the thermal conductivity and specific heat of nanofluids by MD method and found that the MD results are in good agreement with the experimental data. Sun et al. (2011) performed molecular dynamics simulations to calculate the thermal conductivity of nanofluid in shear field and showed that the nanoparticle rotates under the action of the velocity gradient. Lv et al. (2011) and Cui et al. (2012) simulated the flow behaviors of nanofluids between flat plates under shear flow condition. The results showed that the nanoparticles would translate and rotate besides main flowing and these motions could enhance micro-flow in nanofluids. In summary, MD simulation can be used to describe the interactions between the two phases in nanofluids effectively, while there are few MD calculations on the flow behaviors of nanofluids and lack of detailed description on the flow field.

In light of the above, two physical models which are the near-wall model and main flow model will be built in this paper according to the characteristics of macro-flow. The flow behaviors of nanofluids in the two models will be calculated by MD method. Unlike the previous studies, the effect of wall on the motion of nanoparticles and the flow behaviors of nanofluids in the main flow model are investigated. The slip velocity between the nanoparticle and base fluid and the velocity fluctuation of base fluid are also considered in this paper. The aim of the paper is to obtain a comprehensive understanding of nanofluids flowing and offer theory guidance for macro-calculation.

2 Simulation methods

2.1 Model setup

The simulations were carried out with the classical open source molecular dynamic LAMMPS code (Plimpton 1995). The MD simulation systems are shown in Fig. 1. Figure 1a shows the model system of near-wall model, where the periodic boundary conditions are imposed in the x - and z -directions. The simulation box is $8 \times 9.2 \times 8 \text{ nm}^3$ in size, and the liquid height is $h = 8 \text{ nm}$. The distance between nanoparticle and the wall is d . The nanoparticle is free to move in the x - and y -direction, and the parameter d is the average of the distance (y -direction) between the nanoparticle and the wall in calculation. The lowest layer of the wall is frozen, and the wall is fixed. The main flow model system is shown in

Fig. 1 MD simulation systems. **a** Near-wall model. **b** Main flow model

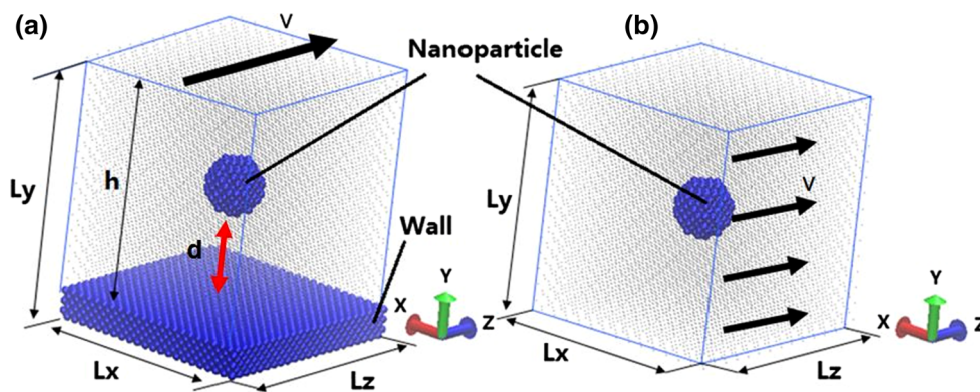


Fig. 1b. The unit cell size is $8 \times 8 \times 8 \text{ nm}^3$. Periodic boundary conditions are imposed in the x -, y - and z -directions. The two models are both contain one nanoparticle with diameter of 2 nm. The material of nanoparticles and wall is copper. In order to simplify calculations, liquid argon is selected as the base fluid. The total amount of atoms in the near-wall model is 17,051. The wall is constructed by 5,808 atoms. The number of atoms in the main flow model is 11,235. Initially all the atoms of liquid argon, copper nanoparticles and wall are arranged as face-centered cubic lattice (FCC).

2.2 Molecular dynamics

Molecular dynamics is a method of deterministic computer simulation. It regards microscopic particles in the simulate system as research objects (Allen and Tildesley 1987). Successive configurations of the system are generated by integrating Newton’s laws of motion. The result is a trajectory that specifies how the velocities and positions of the particles in the system vary with simulation time (Leach 2001). The force field is used to simulate the interactions of atoms. The equations of motion of particles are shown in Eq. (1).

$$\begin{cases} m_i \frac{\partial \mathbf{v}_i}{\partial t} = \mathbf{F}_i(t) = -\frac{\partial U}{\partial \mathbf{r}_i} + \dots \\ \dot{\mathbf{r}}(t) = \mathbf{v}(t) \end{cases} \quad (1)$$

where m_i and \mathbf{v}_i are the mass and velocity of particle, respectively, and t is the time, $\mathbf{F}_i(t)$ is the force exerted on the particles, U is the potential function, \mathbf{r}_i is the coordinate of particle, and the subscript i is the number of particle. In molecular dynamics, finite difference techniques are used to solve the Newtonian motion equations.

In our simulations, the interatomic interactions between argon atoms and those between copper and argon atoms are described by Lennard-Jones potential (Sun et al. 2011) as shown in Eq. (2).

$$U(r_{ij}) = 4\epsilon \left[\left(\frac{\sigma}{r_{ij}} \right)^{12} - \left(\frac{\sigma}{r_{ij}} \right)^6 \right] \quad (2)$$

where ϵ and σ are energy parameter and length scale, respectively, and r_{ij} is the intermolecular distance between atoms i and j . For argon, $\epsilon = 1.67 \times 10^{-21} \text{ J}$ and $\sigma = 0.3405 \text{ nm}$, and for copper, $\epsilon = 65.625 \times 10^{-21} \text{ J}$ and $\sigma = 0.23377 \text{ nm}$. The Lorentz–Berthelot mixing rule (Allen and Tildesley 1987) is used to determine parameters between argon and copper atoms, which is written as:

$$\epsilon_{sl} = \sqrt{\epsilon_{ss} \cdot \epsilon_{ll}} \quad (3)$$

$$\sigma_{sl} = \frac{\sigma_{ss} + \sigma_{ll}}{2} \quad (4)$$

where s and l denote solid and liquid, respectively. Therefore, σ and ϵ between argon and copper are 0.2871 nm and $10.4153 \times 10^{-21} \text{ J}$, respectively.

More precise embedded atom method (EAM) potential (Foils et al. 1986) shown in Eq. (5) is used to represent interactions between copper atoms,

$$U = \sum_i F_i \left(\sum_{j \neq i} \rho_j(r_{ij}) \right) + \frac{1}{2} \sum_{j \neq i} \phi_{ij}(r_{ij}) \quad (5)$$

where F_i is the embedding energy which is a function of the atomic electron density ρ , ϕ is a pair potential interaction, and i and j represent atoms i and j , respectively.

2.3 Simulation procedure

The initial positions of all the atoms are arranged in a regular FCC lattice, so the system needs to be relaxed adequately firstly in order to let the system reach equilibrium state. In the process of relaxation, the temperature of simulation system is fixed to be 86 K to make the low-boiling liquid argon to remain liquid. In this study, the near-wall model is relaxed for 400 ps and the system reaches equilibrium state. Next, a shear velocity in the z -direction is added to the top layer of fluid, and the near-wall shear flow is formed. For the main

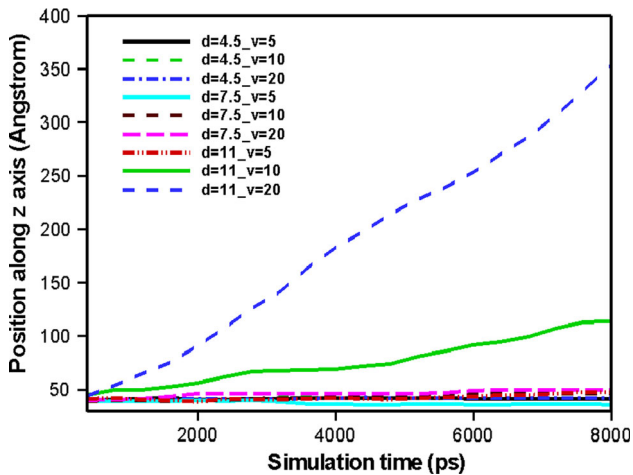


Fig. 2 Positions of nanoparticle along z -direction as function of simulation time

flow model, the relaxation process is the same as that of near-wall model. After relaxation, a uniform velocity in the z -direction is assigned to all of the base fluid atoms and the nanoparticle is moving forward with the base fluid. After the shear velocity and uniform velocity are assigned to the near-wall model and main flow model, respectively, the two models are equilibrated for 400 ps again. Finally, each model is simulated for 8,000 ps to obtain enough data used for statistically calculating physical properties. The reason for the statistical time of 8,000 ps is that the flow behaviors of nanofluids and the motion of nanoparticle can be observed and the observations are reproducible. In order to make the simulations have the same number of statistics and consistent, the statistical time for the two considered models is the same. The simulation time step length is 0.002 ps. NVE ensemble is used in the simulations of the two models where total number of system atoms N , system volume V and system energy E are constant throughout the simulation. In this study, the velocity Verlet (Swope et al. 1982) algorithm is used for calculation of atomic motions, which is written as:

$$\mathbf{r}_i(t + \delta t) = \mathbf{r}_i(t) + \mathbf{v}_i(t)\delta t + \frac{1}{2m}\mathbf{F}_i(t)\delta t^2 \quad (6)$$

$$\mathbf{v}_i(t + \delta t) = \mathbf{v}_i(t) + \frac{1}{2m_i}[\mathbf{F}_i(t + \delta t) + \mathbf{F}_i(t)]\delta t \quad (7)$$

where δt is the time interval.

3 Results and discussion

3.1 Flow behaviors in the near-wall model

To research the effect of wall on the motion state of nanoparticle, four cases are simulated, which are $d = 4.5$, $d = 7.5$, $d = 11$ and $d > 11$ Å. Each case is simulated

under different shear velocities of 5, 10 and 20 m/s. The flow of pure fluid argon (without nanoparticle) is also computed in this paper.

In Fig. 2, the positions of nanoparticles along the z -direction are shown. When the distance between the nanoparticle and wall is 4.5 and 7.5 Å, respectively, the displacement of nanoparticle in the direction of flow is almost zero under three shear velocities. Only when the value of d is increased to 11 Å and the shear velocity is higher than 5 m/s, nanoparticle begins to move along z -axis.

The interactive force between the nanoparticle and wall was calculated in this paper, and the result is zero, so the phenomenon that nanoparticle which is very close to the wall does not move with liquid argon is not caused by the absorption of the wall on the nanoparticle. Figure 3a and b shows the number density profile of pure fluid argon normal to the wall and the distributions of the number density of argon atom around the nanoparticle, respectively. As shown in Fig. 3a, there exist argon adsorbent layers near the wall, which is named solid-like layer (Granick 1991). The calculation method for number density in Fig. 3b is shown in Eq. (8).

$$n = \frac{\Delta N}{\Delta V} \quad (8)$$

where ΔN is number of atoms within the volume ΔV . The computational domain around nanoparticle is divided into many spherical shells, and the volume of a sphere shell is ΔV . The place where the value of R is zero is the surface of nanoparticle. From Fig. 3b, it can be seen that the number density of argon near the nanoparticle surface is much higher than elsewhere, which indicates that adsorbed layers are formed around the nanoparticle. Similar results were also observed by Li et al. (2008) and Lv et al. (2011). When the nanoparticle is very close to the wall, the solid-like layer near the wall will overlap with the adsorbed layer around nanoparticle, as shown in Fig. 4, which makes the nanoparticle not move with the liquid argon.

The rotation of nanoparticle is also computed in this paper. Figure 5 shows the angular velocity components of nanoparticle at different simulation times. The angular velocity components are averaged every 400 ps, namely the angular velocity component quantity on 400 ps is the average from zero to 400 ps, and so on. When the nanoparticle is very close to the wall ($d = 4.5$ Å), the nanoparticle still rotates quickly, but the angular velocity is significantly lower than that of the nanoparticle which is far away from the wall ($d > 11$ Å). By comparing Fig. 5d, e and f, it is found that the angular velocity component quantity in the x -direction is much higher than in the other two directions. And the higher the shear velocity, the faster the rotation of the nanoparticle. This is due to the velocity

Fig. 3 **a** Number density profile of pure fluid argon normal to the wall. **b** Distributions of the number density of argon atom around nanoparticles

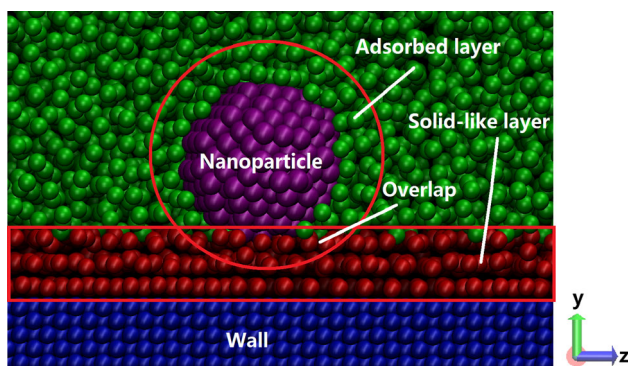
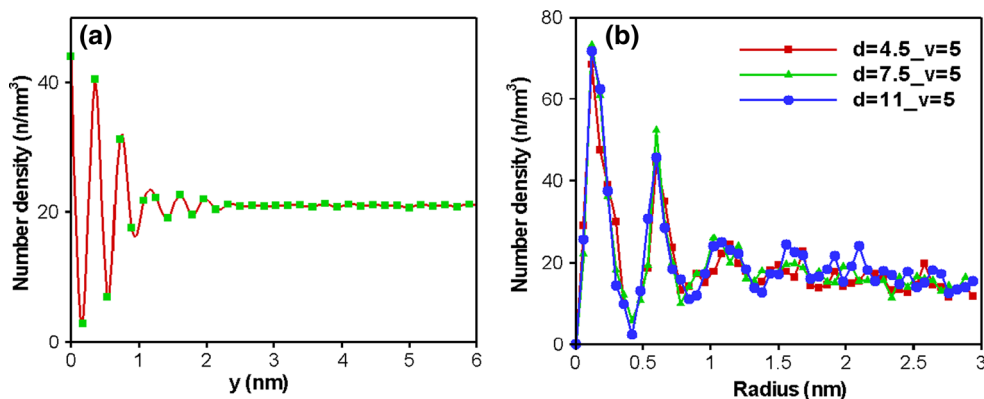


Fig. 4 Solid-like layer near the wall and adsorbed layer around nanoparticle

gradient along the y -axis, and the velocity of atoms of nanoparticle upper surface is different from that of lower surface.

Nanoparticles also translate during the simulations. Figure 6 shows the changes of the nanoparticle’s position in the x -direction and y -direction under different shear velocities. The distance between the nanoparticle and the wall exceeds 11 \AA , and there is no overlap between the solid-like layer near the wall and the adsorbed layer around the nanoparticle. The results indicate that the nanoparticle has translation in the other two directions besides main flowing. Nanoparticle’s translation in the x -direction is larger than that in the y -direction. When the shear velocity is increased, the variation range of nanoparticle’s position does not have obvious regularity. For the fourth case ($d > 11 \text{ \AA}$) where there is no overlap between the solid-like layer near the wall and the adsorbed layer around the nanoparticle, the nanoparticle’s displacement in the y -direction changes within a large range. Furthermore, with the change of the shear velocity, the displacement of nanoparticle in the y -direction changed, as shown in Fig. 6b. The averages of the distance between the nanoparticles and the wall are not the same for the three shear velocities of 5, 10 and 20 m/s. Therefore, there is not a

certain value of d that could be used to represent the fourth case and $d > 11 \text{ \AA}$ is chosen.

Based on above analysis, we can get an overview of the flow state of nanofluids in the near-wall model. When the nanoparticle is very close to the wall, the rotation and translation of nanoparticle are inhibited to some extent. Nevertheless, the nanoparticle still rotates quickly near the wall. When the nanoparticle is far away from the wall ($d > 11 \text{ \AA}$), the nanoparticle not only has rotation motion, but also has translation.

3.2 Flow behaviors in the main flow model

The main flow system is simulated 5 times under different flow velocities of 1, 5, 10, 20 and 40 m/s. The flow behaviors of nanofluids and pure fluid argon are both simulated in this paper.

The angular velocity components of nanoparticle in the main flow model are shown in Fig. 7. The statistical method of the angular velocity is the same as before. As shown in the figures, the rotation of nanoparticles is irregular and the fluctuation ranges of the three angular velocity components are similar. When the flow velocity is changed, the magnitude of angular velocity has no obviously change.

Figure 8a and b shows the changes of nanoparticle’s position with simulation time in the x -direction and y -direction, respectively. It can be seen that the nanoparticle in the main flow model would also translate in the other two directions besides main flowing. The variation range of nanoparticle’s position has no obvious regularity with the change in the flow velocity.

3.3 Slip velocity between nanoparticles and the liquid argon

Nanofluid is actually a solid–liquid fluid. Wang et al. (2013) and He et al. (2009) believed that the flow and heat transfer characteristics of nanofluids could be better

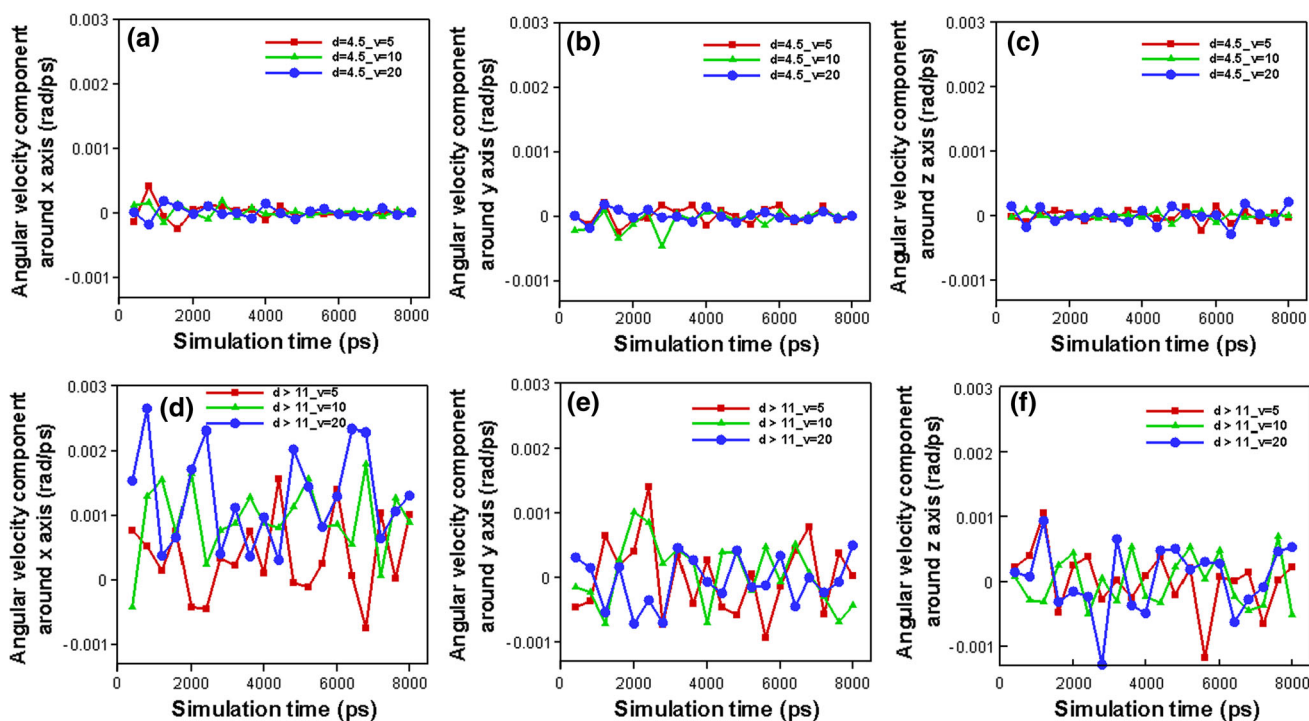


Fig. 5 Angular velocity components of nanoparticles under different shear velocities. **a**, **b** and **c** show angular velocity component around x -, y - and z -direction, respectively, for the case of $d = 4.5 \text{ \AA}$. **d**, **e** and

f show angular velocity component around x -, y - and z -direction, respectively, for the case of $d > 11 \text{ \AA}$

Fig. 6 Translational components along x - (**a**) and y -axis (**b**) for the case of $d > 11 \text{ \AA}$ under different shear velocities

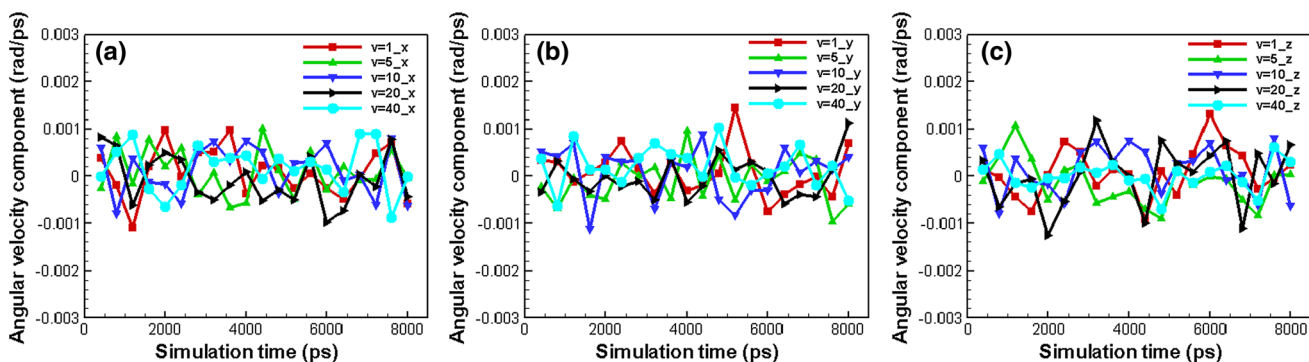
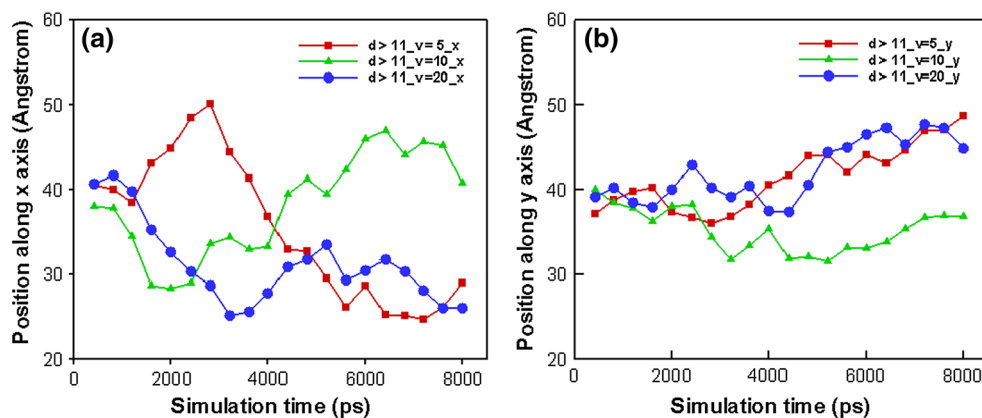


Fig. 7 Angular velocity components of nanoparticles along x - (**a**), y -axis (**b**) and z -axis (**c**) under different flow velocities

Fig. 8 Translational components along *x*- (a) and *y*-axis (b) under different flow velocities

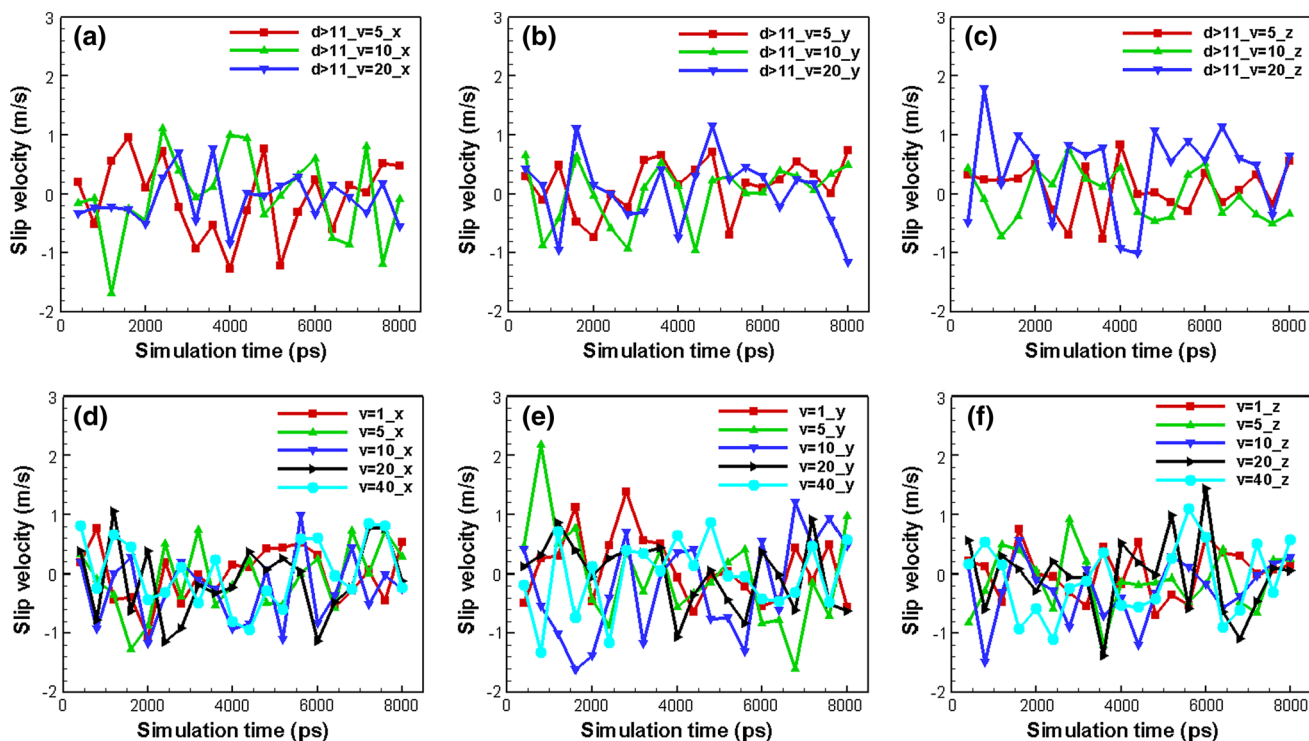
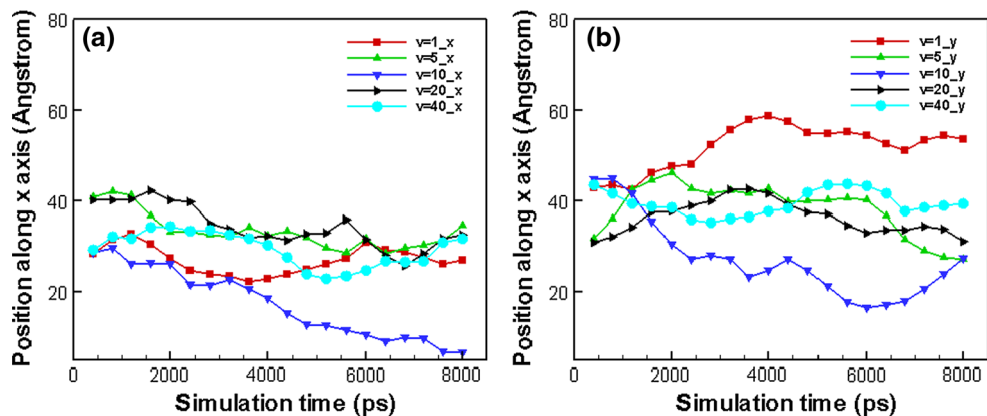


Fig. 9 Slip velocities between nanoparticles and liquid argon. a, b and c show slip velocity component in *x*-, *y*- and *z*-direction, respectively, in the near-wall model ($d > 11 \text{ \AA}$). d, e and f show slip velocity component in *x*-, *y*- and *z*-direction, respectively, in the main flow model

predicted by taking the interactions between the two phases into consideration. However, there is lack of adequate theoretical supports for this viewpoint. When the nanoparticle is very close to the wall, there exist slip velocity between the two phases and the nanofluids display the properties of two-phase flow. Figure 9 shows the slip velocities between the nanoparticle and liquid argon. The slip velocity is obtained by Eq. (9).

$$\Delta v_s = v_p - v_f \tag{9}$$

where Δv_s is the slip velocity between the two phases, v_p is the velocity of nanoparticle and v_f is the velocity of liquid argon. The near-wall model in which the nanoparticle is far

away from the wall ($d > 11 \text{ \AA}$) and the main flow model are both considered. As can be seen from the figures, the inter-phase velocity slip always exists in the three-dimensional coordinates and cannot be ignored. The slip velocity components have both positive and negative values, which indicate that the interaction between the two phases is complex. Thus, it can be seen that the flow behaviors of nanofluids in the two models display the typical characteristics of two-phase flow. In addition, the interactions between the two phases should be considered when the flow and heat transfer of nanofluids are studied by computational fluid dynamics (CFD) method. The magnitude of inter-phase velocity slip in the near-wall model is similar to

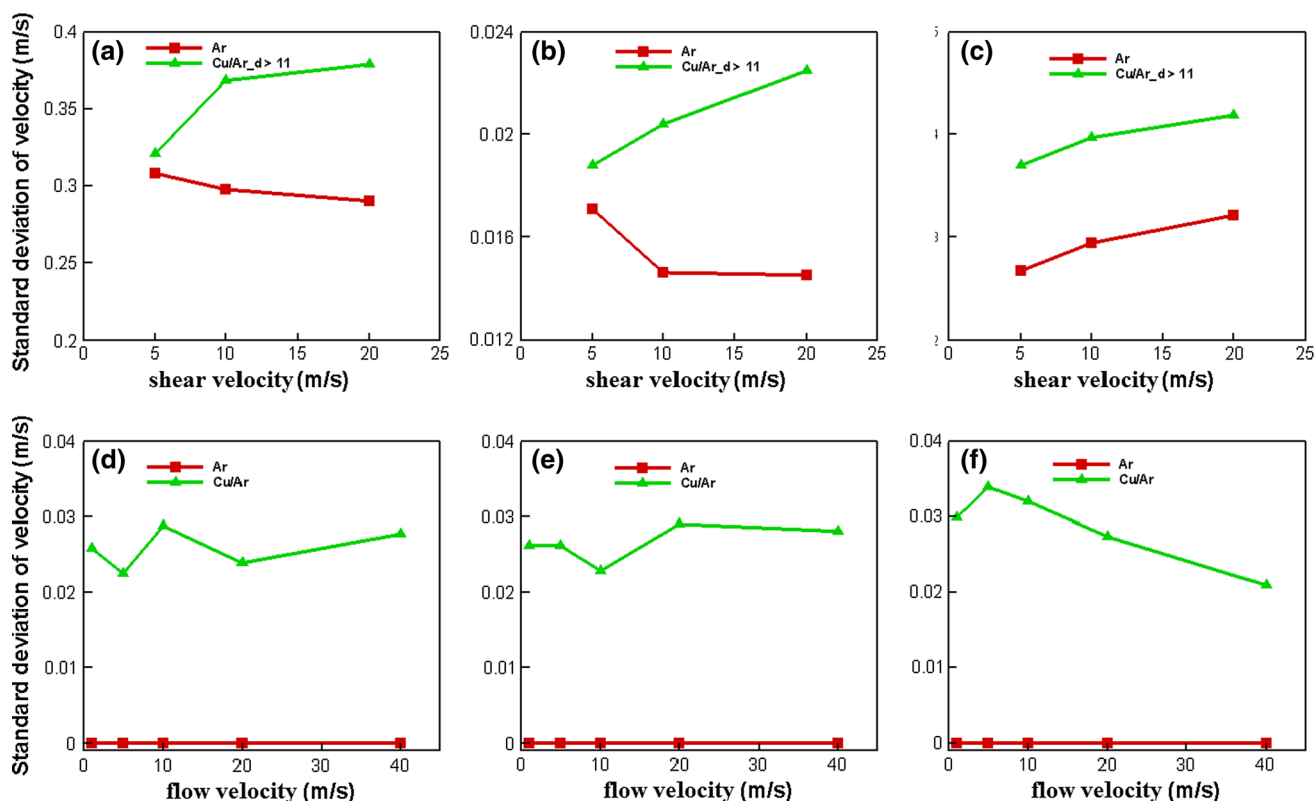


Fig. 10 Velocity fluctuations of pure liquid argon and nanofluids. **a**, **b** and **c** show velocity fluctuations along x -, y - and z -direction in the near-wall model ($d > 11 \text{ \AA}$), respectively. **d**, **e** and **f** show velocity fluctuations along x -, y - and z -direction in the main flow model, respectively

that in the main flow model. As the shear velocity increased, the ranges of slip velocity remain unchanged as show in Fig. 9a, b and c. Similar results are also observed in the main flow model.

3.4 Velocity fluctuations of the base fluid

Rotation and translation of nanoparticles affect the flow behaviors of fluid around nanoparticles, thus those of the whole flow region are influenced. Furthermore, the slip velocity between the nanoparticles and base fluid would enhance the exchange of momentum. Therefore, the velocity fluctuation of nanofluids would be different with that of the pure base fluid. Figure 10 shows the comparisons of velocity fluctuations between nanofluids and the pure base fluid. The calculation method of velocity fluctuation is the same as that of the standard deviation of the velocity. The velocities that are calculated every 400 ps are used as samples. It is clearly observed that the velocity fluctuations of nanofluids are much higher than that of the pure base fluid, whether in the near-wall model or main flow model. This is one of the reasons for heat transfer enhancement in nanofluids.

4 Conclusions

The objective of this work is to get an overall understanding of flow characteristics of nanofluids. The near-wall model and main flow model were built, and the flow behaviors of nanofluids in the two models were studied by MD method. The following conclusions have been obtained:

1. When the nanoparticle is very close to the wall, the nanoparticle would not move with the liquid argon. This result can be explained in terms of the overlap of the solid-like layer near the wall with the adsorbed layer around the nanoparticle. When the nanoparticle is far away from the wall ($d > 11 \text{ \AA}$), the nanoparticle not only has rotation motion, but also has translation. For the main flow model, the nanoparticle would rotate and translate besides main flowing.
2. There was slip velocity between nanoparticles and liquid argon no matter in the near-wall model or main flow model. The flow characteristics of nanofluids display typical features of two-phase flow. The range of slip velocity is not sensitive to the change of flow velocity. Because of the irregular motions of

nanoparticles and the slip velocity between the two phases, the velocity fluctuation in nanofluids is enhanced.

Acknowledgments This work is supported by National Natural Science Foundation of China (Grant No. 51276031 and 51006015) and the Fundamental Research Funds for the Central Universities (Grant No. DUT11RC(3)37).

References

- Allen MP, Tildesley DJ (1987) Computer simulation of liquids. Clarendon Press, Oxford
- Beiki H, Esfahany MN, Etesami N (2013) Turbulent mass transfer of Al_2O_3 and TiO_2 electrolyte nanofluids in circular tube. *Microfluid Nanofluid* 15:501–508
- Bianco V, Chiacchio F, Manca O, Nardini S (2009) Numerical investigation of nanofluids forced convection in circular tubes. *Appl Thermal Eng* 29:3632–3642
- Choi SUS (1995) Enhancing thermal conductivity of fluids with nanoparticles. In: Siginer DA, Wang HP (eds) *Developments and applications of non-newtonian flows*. ASME, New York, pp 99–103
- Cui WZ, Bai ML, Lv JZ, Zhang L, Li GJ, Xu M (2012) On the flow characteristics of nanofluids by experimental approach and molecular dynamics simulation. *Exp Therm Fluid Sci* 39:148–157
- Duangthongsuk W, Wongwises S (2010) An experimental study on the heat transfer performance and pressure drop of TiO_2 -water nanofluids flowing under a turbulent flow regime. *Int J Heat Mass Transfer* 53:334–344
- Eapen J, Li J, Yip S (2007) Mechanism of thermal transport in dilute nanocolloids. *Phys Rev Lett* 98:028302
- Foils SM, Baskes MI, Daw MS (1986) Embedded-atom-potential functions for the fcc metals Cu, Ag, Au, Ni, Pd, Pt and their alloys. *Phys Rev B* 33:7983–7991
- Granick S (1991) Motions and relaxation of confined liquids. *Science* 253:374–379
- Haghshenas FM, Esfahany MN, Talaie MR (2010) Numerical study of convective heat transfer of nanofluids in a circular tube two-phase model versus single-phase model. *Int Commun Heat Mass Transfer* 37:91–97
- He YR, Men YB, Zhao YH, Lu HL, Ding YL (2009) Numerical investigation into the convective heat transfer of TiO_2 nanofluids flowing through a straight tube under the laminar flow conditions. *Appl Thermal Eng* 29:1965–1972
- Heris SZ, Esfahany MN, Etemad SG (2007) Experimental investigation of convective heat transfer of Al_2O_3 /water nanofluid in circular tube. *Int J Heat Fluid Flow* 28:203–210
- Ho CJ, Chen WC (2013) An experimental study on thermal performance of Al_2O_3 /water nanofluid in a minichannel heat sink. *Appl Thermal Eng* 50:516–522
- Hwang KS, Jang SP, Choi SUS (2009) Flow and convective heat transfer characteristics of water-based Al_2O_3 nanofluids in fully developed laminar flow regime. *Int J Heat Mass Transfer* 52:193–199
- Jabbarzadeh A, Atkinson JD, Tanner RI (1998) Nanorheology of molecularly thin films of n-hexadecane in Couette shear flow by molecular dynamics simulation. *J Non-New Fluid Mech* 77:53–78
- Jabbarzadeh A, Atkinson JD, Tanner RI (2002) The effect of branching on slip and rheological properties of lubricants in molecular dynamics simulation of Couette shear flow. *Tribol Int* 35:35–46
- Kalteh M, Abbassi A, Saffar-Avval M, Harting J (2011) Eulerian–Eulerian two-phase numerical simulation of nanofluid laminar forced convection in a microchannel. *Int J Heat Fluid Flow* 32:107–116
- Kang H, Zhang Y, Yang M (2011) Molecular dynamics simulation of thermal conductivity of Cu–Ar nanofluid using EAM potential for Cu–Cu interactions. *Appl Phys A* 103:1001–1008
- Leach AR (2001) *Molecular modelling: principles and applications*, 2nd edn. Prentice Hall, London
- Li L, Zhang Y, Ma H, Mo Y (2008) An investigation of molecular layering at the liquid–solid interface in nanofluids by molecular dynamics simulation. *Phys Lett A* 372:4541–4544
- Li L, Zhang Y, Ma H, Mo Y (2010) Molecular dynamics simulation of effect of liquid layering around the nanoparticle on the enhanced thermal conductivity of nanofluids. *J Nanopart Res* 12:811–821
- Liang Z, Tsai HL (2011) Effect of molecular film thickness on thermal conduction across solid–film interfaces. *Phys Rev E* 83:061603
- Lin YS, Hsiao PY, Chieng CC (2011) Roles of nanolayer and particle size on thermophysical characteristics of ethylene glycol-based copper nanofluids. *Appl Phys Lett* 98:153105
- Lv JZ, Cui WZ, Bai ML, Li XJ (2011) Molecular dynamics simulation on flow behavior of nanofluids between flat plates under shear flow condition. *Microfluid Nanofluid* 10:475–480
- Mohebbi A (2012) Prediction of specific heat and thermal conductivity of nanofluids by a combined equilibrium and non-equilibrium molecular dynamics simulation. *J Mol Liq* 175:51–58
- Plimpton SJ (1995) Fast parallel algorithms for short-range molecular dynamics. *J Comp Phys* 117:1–19
- Sarkar S, Selvam RP (2007) Molecular dynamics simulation of effective thermal conductivity and study of enhanced thermal transport mechanism in nanofluids. *J Appl Phys* 102:074302
- Sun C, Lu WQ, Liu J, Bai B (2011) Molecular dynamics simulation of nanofluid's effective thermal conductivity in high-shear-rate Couette flow. *Int J Heat Mass Transfer* 54:2560–2567
- Swope WC, Andersen HC, Berens PH, Wilson KR (1982) A computer simulation method for the calculation of equilibrium constants for the formation of physical clusters of molecules: application to small water clusters. *J Chem Phys* 76:637–649
- Thompson PA, Robbins MO (1990) Shear flow near solids: epitaxial order and flow boundary conditions. *Phys Rev A* 41:6830–6837
- Vladkov M, Barrat JL (2006) Modeling transient absorption and thermal conductivity in a simple nanofluid. *Nano Lett* 6:1224–1228
- Wang P, Bai ML, Lv JZ, Zhang L, Cui WZ, Li GJ (2013) Comparison of multi-dimensional simulation models for nanofluids flow characteristics. *Numer Heat Transfer B* 63:62–83
- Wen D, Ding Y (2004) Experimental investigation into convective heat transfer of nanofluids at the entrance region under laminar flow conditions. *Int J Heat Mass Transfer* 47:5181–5188
- Wen D, Ding Y (2005) Effect of particle migration on heat transfer in suspensions of nanoparticles flowing through minichannels. *Microfluid Nanofluid* 1:183–189
- Xu M, Cui WZ, Bai ML, Bian YN, Zhang L, Lv JZ (2011) Experimental study on flow behavior of SiO_2 -water nanofluids in a wavy-walled tube. *J Exper Fluid Mech* 25:29–34
- Xuan YM, Li Q (2003) Investigation on convective heat transfer and flow features of nanofluids. *ASME J Heat Transfer* 125(1):151–155
- Xuan YM, Roetzel W (2000) Conceptions for heat transfer correlation of nanofluids. *Int J Heat Mass Transfer* 43:3101–3107